Complex Formation between Polyelectrolyte and Oppositely Charged Mixed Micelles: Static and Dynamic Light Scattering Study of the Effect of Polyelectrolyte Molecular Weight and Concentration

Yingjie Li, Jiulin Xia,† and Paul L. Dubin*

Department of Chemistry, Indiana University–Purdue University, Indianapolis, Indiana 46202

Received May 17, 1994; Revised Manuscript Received July 19, 1994®

ABSTRACT: Dynamic light scattering, static light scattering, and turbidimetry were used to investigate the effect of polyelectrolyte molecular weight and concentration on complex formation between a strong polyelectrolyte, poly(dimethyldiallylammonium chloride) (PDMDAAC), and oppositely charged mixed micelles of Triton X-100 (TX100) and sodium dodecyl sulfate (SDS). The hydrodynamic radius (R_h) of the complexes is about twice those of the PDMDAAC from which they are formed, while the radius of gyration (R_g) of the complexes remains essentially unchanged. This suggests that the complex formed is compact. With increasing polyelectrolyte concentration, intrapolymer complexes transform to interpolymer complexes. The interpolymer complexes are not stable and in time phase separate (coacervate). Although the polyelectrolyte molecular weight has only a small effect on the structure of the complex in the intrapolymer complex region, the intra- to interpolymer complex transition depends strongly upon the molecular weight of the polyelectrolyte. The polyelectrolyte concentration at which the transition occurs decreases with increasing polyelectrolyte molecular weight. If the polyelectrolyte molecular weight is low enough, this sharp transition is not observed, and no associative phase separation is observed.

Introduction

Complex formation between polyelectrolytes and oppositely charged surfactants has been a subject of intense research effort for both fundamental and technological reasons.[1–16] Knowledge acquired from the study of polyelectrolyte–surfactant interactions can be applied to important industrial and biological processes. For example, the interaction of polyelectrolytes with oppositely charged micelles may serve as a useful model system for polyion–colloid systems. Such systems are represented in a wide range of situations including water purification and precipitation of bacterial cells with polycations[17] and the stabilization of preceramic suspensions.[18] In the biological realm, they are central to the immobilization of enzymes in polyelectrolyte complexes[19] and the purification of proteins by selective precipitation and coacervation.[20–23] The fundamental interactions that govern the nonspecific association of DNA with basic proteins[24,25] must also be identical to the ones that control the binding of charged colloids to oppositely charged polyelectrolytes.

Until recently, most of the published studies on polyelectrolyte–surfactant complexes involved surfactants at such a low concentration that free micelles do not exist in the system, mainly because of the difficulties arising from phase separation. The interaction between polyelectrolytes and oppositely charged surfactants is dominated by strong electrostatic forces, although hydrophobic interactions may play a secondary role.[2,3,5,8] These forces cause the association to start at a very low surfactant concentration, known as the critical aggregation concentration (cac), which is usually a few orders of magnitude lower than the critical micelle concentration (cmc) of the free surfactant. Unlike the situation for nonionic polymer–ionic surfactant systems, the complex usually cannot coexist with free micelles because precipitation is observed as the addition of ionic surfactant brings the polyelectrolyte close to charge neutralization.[26,27] Therefore, phase separation effects result in the restriction of most studies of strong polyelectrolytes with oppositely charged surfactants to surfactant concentrations below or not much higher than the cmc.

Dubin and co-workers[28–36] have demonstrated that the strong electrostatic interaction could be attenuated by using mixed micelles of nonionic and ionic surfactants. Thus Dubin and Oteri[28] showed that the interaction between poly(dimethyldiallylammonium chloride) (PDMDAAC) and mixed micelles of sodium dodecyl sulfate (SDS) and Triton X-100 (TX100) takes place only when a critical molar ratio Y_c of SDS to TX100 has been reached, where Y is defined as Y = [SDS]/([SDS] + [TX100]), and is proportional to the average mixed micelle surface charge density. In addition to the phase transition at Y_c corresponding to the reversible formation of soluble polyelectrolyte–mixed micelle complexes, Dubin and Oteri[28] observed a second phase transition, corresponding to bulk phase separation, at a higher Y value, denoted by Y_p. Y_p usually exceeds Y_c by about 50–100%. The region between Y_c and Y_p represents a range of micelle surface charge density where soluble, reversible complexes could form. At moderate or high polyelectrolyte concentration, a maximum in the turbidity versus Y curve is observed between Y_c and Y_p. The soluble complex formation as well as its dependence upon ionic strength, polyelectrolyte concentration, and surfactant concentration has been studied by Dubin and co-workers using a variety of techniques.

One parameter that has received relatively little attention in studies of polyelectrolyte–surfactant complex formation is the polyelectrolyte molecular weight.[37] Using turbidimetry, Dubin *et al.*[33] indicated that the molecular weight of PDMDAAC did not exhibit a significant effect on PDMDAAC/TX100–SDS complex formation but did observe that Y_c decreased slightly with increasing molecular weight of poly(sodium styrenesulfonate)

* To whom correspondence should be addressed.
† Current address: Life Technologies, Inc., P.O. Box 6009, Gaithersburg, Maryland 20884-9980.
® Abstract published in *Advance ACS Abstracts*, October 15, 1994.

0024-9297/94/2227-7049$04.50/0

(NaPSS), in the presence of mixed micelles of TX100 and dodecyltrimethylammonium bromide.[39] Lindman and co-workers[40] studied the effect of polyelectrolyte molecular weight on the phase behavior of mixtures of alkyltrimethylammonium bromide (C_nTAB) and the anionic polysaccharide hyaluronic acid. The tendency toward phase separation increased slightly with increasing polyelectrolyte molecular weight; only a slight change was observed in the phase diagram. Recently, Choi and Kim[41] studied the interaction between poly(acrylic acid) (PAA) and C_nTAB. Their fluorescence measurements indicated a lower cac for higher molecular weight PAA. Also of possible relevance are studies of the role of polyelectrolyte molecular weight on the precipitation of proteins with polyelectrolytes:[42-45] generally, high molecular weight leads to high recoveries of proteins.

Polymer–micelle complexes have been described by Cabane and Duplessix as a "necklace of beads".[46] However, this model may break down if the size of micelles becomes similar to that of the polymer, resulting from either a decrease in the length of polymer or an increase in the size of micelles. For example, if the size of polymer is even smaller than that of micelles, adsorption might be a more proper term for describing the phenomena. The finite size of micelles will certainly affect the structure of complexes via the excluded volume effect. It is thus interesting to study the change of complex formation as the size of one of the components, polymer or micelle, changes. PDMDAAC/TX100–SDS should be a good candidate since the hydrodynamic radius (R_h) of the free micelles could reach *ca.* 50 nm,[47] while the range of R_h for available PDMDAAC fractions is around 4.5–26 nm.[48]

A second interesting parameter in polyelectrolyte–surfactant complex formation is polyelectrolyte concentration (C_p), expressed in this paper as the weight ratio of PDMDAAC to surfactant. This parameter is usually a determining factor for intra- *vs* intercomplex formation. Dubin and co-workers[34-36] have indicated that an intrapolymer complex forms in the PDMDAAC/TX100–SDS system at low C_p, while at high C_p, an interpolymer complex could form. However, the PDMDAAC used in those studies was polydisperse. Since polyelectrolyte molecular weight could influence intra- *vs* interpolymer complex formation, narrow molecular weight distribution samples should be preferable in such studies. In addition, it is particularly interesting to see if an interpolymer complex is the precursor of phase separation.

A series of PDMDAAC fractions with narrow molecular weight distribution has been obtained by preparative gel permeation chromatography (GPC).[48] These fractions were characterized by static and dynamic light scattering, viscosity, GPC, and electrophoretic light scattering. In the present study we explore the effect of polyelectrolyte molecular weight and concentration on PDMDAAC/TX100–SDS complex formation.

Experimental Section

Materials. A commercial sample of PDMDAAC, Merquat 100 from Calgon Corp. (Pittsburgh, PA), with a nominal molecular weight of 200K and polydispersity of $M_w/M_n \sim 10$ was fractionated via preparative GPC, and the fractions were characterized by static and dynamic light scattering, viscosity, GPC, and electrophoretic light scattering.[48] Table 1 shows the molecular characteristics of the PDMDAAC fractions used in this study. TX100 was purchased from Aldrich and SDS from Fluka. Ionic strength was adjusted by using NaCl from Fisher. Milli-Q water was used throughout this work. TX100, SDS, and NaCl were used without further purification.

The Merquat 100 sample used in this study was dialyzed through a membrane with a nominal 12K–14K cutoff. Therefore, it is expected that the molecular weight distribution index M_w/M_n should be much smaller than 10.

Table 1. Description of the PDMDAAC Fractions Used in This Study

fraction no.	$10^{-3}M_w$[a,b]	fraction no.	$10^{-3}M_w$[a,b]
2	1400	19	110
3	1300	23	50
8	590	27	22
15	200		

[a] M_w values were obtained from GPC measurements on a Superose 6 column with a flow rate of 0.53 mL/min. NaAc/HAc buffer was used to maintain the pH at 5.2. NaCl was used to adjust the total ionic strength to 0.5 M. The column was calibrated with PDMDAAC standards.[48] [b] Polydispersity (M_w/M_n) of all the fractions is around 1.2.

Turbidimetry. Turbidity measurements were performed at 420 nm using a Brinkmann PC800 probe colorimeter equipped with a 2-cm path length fiber optics probe. "Type I" titrations were performed at 24 ± 1 °C by adding 60 mM SDS in 0.40 M NaCl to a solution of 40 mM TX100 and 0.6 g/L PDMDAAC, also in 0.4 M NaCl. 100% T was recorded. All measured values were corrected by subtracting the turbidity of a polymer-free blank.

Dynamic Light Scattering. The type I titration procedure was followed to bring Y to 0.30. Such solutions were diluted 10 times by using 0.40 M NaCl, to yield final solutions with a typical C_p value of [PDMDAAC] = 0.0466 g/L (unless otherwise indicated) and [TX100] = 3.11 mM (fixed throughout this study). Since the cmc of TX100–SDS mixed micelles is expected to be less than 0.2 mM, i.e., at least 15 times smaller than the surfactant concentrations employed here, the system we studied is a polyelectrolyte–*micelle* system. The diluted solutions were passed through 0.45-μm filters (Life Science Products). Most of the dynamic light scattering measurements were carried out at 24 ± 1 °C and at angles from 45 to 120° using a Brookhaven Instruments system equipped with a 72-channel digital correlator (BI-2030AT) and an Omnichrome air-cooled 200 mW argon ion laser operating at a wavelength in vacuum λ_0 = 488 nm.

In the self-beating mode of dynamic light scattering, the measured photoelectron count autocorrelation function $G^{(2)}(\tau,q)$ for a detector with a finite effective photocathode area has the form[49-51]

$$G^{(2)}(\tau,q) = N_s\langle n\rangle^2(1 + b|g^{(1)}(\tau,q)|^2) \quad (1)$$

where $g^{(1)}(\tau,q)$ is the first-order scattered electric field (E_s) time correlation function; τ, the delay time; $\langle n\rangle$, the mean counts per sample; N_s, the total number of samples; A ($=N_s\langle n\rangle^2$), the base line; b, a spatial coherence factor depending upon the experimental setup and taken as an unknown parameter in the data fitting procedure; and $q = (4\pi n/\lambda_0)\sin(\theta/2)$, with n and θ being the refractive index of the scattering medium and the scattering angle, respectively.

For a solution of polydisperse particles, $g^{(1)}(\tau,q)$ has the form[49]

$$|g^{(1)}(\tau,q)| = \int_0^\infty G(\Gamma,q)e^{-(\Gamma(q)\tau}\,d\Gamma \quad (2)$$

where $G(\Gamma,q)$ is the normalized distribution of line width Γ measured at a fixed value of q. In the present study, a CONTIN algorithm was used to obtain the average Γ and its distribution of the complex mode and the free micelle mode.[52]

The average line width Γ_{av} at a finite concentration C and a finite value of q is related to the translational diffusion coefficient at infinite dilution and $q \to 0$ extrapolation, D_0, by[53]

$$\Gamma_{av} = D_0q^2(1 + fR_g^2q^2)(1 + k_dC) \quad (3)$$

where f is a dimensionless number which depends upon the chain structure, polydispersity, and solvent quality; R_g is the radius of gyration; and k_d is an average system-specific second virial (diffusion) coefficient which combines the hydrodynamic and thermodynamic factors. Therefore, to get D_0, both extrapolations

of $C \rightarrow 0$ and $q \rightarrow 0$ are required. The hydrodynamic radius, R_h, can then be obtained by using the Stokes–Einstein relation

$$D_0 = k_B T/(6\pi\eta R_h) \quad (4)$$

where k_B is the Boltzmann constant; T is the absolute temperature; and η is the solvent viscosity.

In the present study, only one concentration is used because it is not known to what extent dilution could affect the structure of the complex. No extrapolation to infinite dilution was performed. Therefore, the R_h values presented in this paper are only apparent values. However, the concentration of PDMDAAC in this study is fairly low (typical value 0.0466 g/L). Therefore the lack of concentration extrapolation should not introduce a significant error.

Static Light Scattering. If we take the PDMDAAC/TX100–SDS complex as a solute and the free (unbound) TX100–SDS mixed micelles in 0.4 M NaCl as a solvent (the concentration of the free micelles, although in large excess when compared with PDMDAAC, is not known in the present study), the excess Rayleigh ratio $R(q)$ of the complex at finite q and finite complex concentration C_x has the form[49]

$$HC_x/R(q) = (1/M_{w,x})(1 + R_g^2q^2/3) + 2A_2C_x \quad (5)$$

where $M_{w,x}$ is the weight-averaged molecular weight of the complex; A_2 is the second virial coefficient; and $H = 4\pi^2n^2(dn/dc)^2/(N_A\lambda_o)$, with dn/dc and N_A being the refractive index increment and Avogadro's number, respectively.

The low concentration of PDMDAAC in this study justifies the approximation

$$HC_x/R(q) \approx (1/M_{w,x})(1 + R_g^2q^2/3) \quad (6)$$

Equation 6 can be rearranged to

$$H'C_x/I(q) \approx (1/(M_{w,x}(dn/dc)^2))(1 + R_g^2q^2/3) \quad (7)$$

where $I(q)$ is the excess scattered intensity of the complex and H' is a constant. Therefore, R_g can be estimated from (3 × slope/intercept)$^{1/2}$ in a plot of $1/I(q)$ *vs* q^2.

In the limit of $q \rightarrow 0$, eq 7 can be written as

$$I(q \rightarrow 0) \approx H'C_xM_{w,x}(dn/dc)^2 \quad (8)$$

It is further assumed that $C_x = \beta C_p$, where β is the degree of binding, i.e., the mass of surfactant bound per unit mass polyelectrolyte (this assumption should be reasonable if TX100–SDS is in large excess). Then eq 8 can be written as

$$I(q \rightarrow 0) \approx H'\beta C_pM_{w,x}(dn/dc)^2 \quad (9)$$

Therefore, in a plot of $I(q \rightarrow 0)$ *vs* C_p, if the slope is changed it implies $M_{w,x}$ and/or dn/dc is changed. For example, if interpolymer complexes start to form with increasing C_p, an increased slope change should be observed.

Static light scattering measurements were performed at 24 ± 1 °C and at angles from 25° to 145° along with dynamic light scattering measurements on the same solutions as described above. The excess scattered intensity from complexes was estimated by subtracting the scattered intensity of TX100–SDS micelles without PDMDAAC and at the same concentration as in the PDMDAAC/TX100–SDS system. This disregards the fact that some micelles are bound to PDMDAAC. However, since the surfactant was in excess, i.e., the weight ratio of surfactant to PDMDAAC, $w_{surfactant}/w_{PDMDAAC}$, is generally greater than 30, this approximation may be reasonable. Further evidence supporting this approximation can be found in the Results and Discussion. All the excess scattered intensity values presented in this paper are from extrapolation $q \rightarrow 0$.

Results and Discussion

Figure 1 shows the results from type I titrations in 0.4 M NaCl. The shapes of the curves are very similar to previous results using polydisperse PDMDAAC samples.[33] No turbidity increase is observed until Y reaches Y_c = 0.23, regardless of the PDMDAAC molecular weight. Above Y_c, soluble complex starts to form. When Y reaches Y_p (around 0.38–0.42), phase separation occurs. The curves for 200K < M_w show maxima between Y_c and Y_p. Y_p is also little affected by the PDMDAAC molecular weight. Such phenomena suggest that the initial complex formation process at Y_c mainly involves short polymer segments, although the structure of the complex as detected from more sensitive light scattering techniques may be dependent upon PDMDAAC molecular weight as discussed later. It is noted that the changes in the titration curves with increasing PDMDAAC molecular weight are very similar to those observed with increasing PDMDAAC concentration;[36] i.e., 100 − %T is increased with either increasing polyelectrolyte molecular weight or increasing polyelectrolyte concentration. This can be understood from eq 8, which indicates that the scattered intensity is proportional to both concentration and molecular weight of the complex.

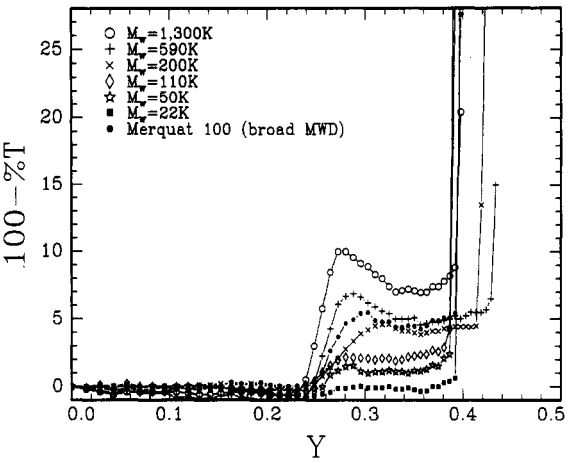

Figure 1. "Type I" turbidity titrations using narrow molecular weight distribution PDMDAAC fractions ([PDMDAAC] = 0.6 g/L) with [TX100] = 40 mM, [SDS] = 60 mM, and [NaCl] = 0.4 M.

One noticeable feature in Figure 1 is that the maximum is only obvious when PDMDAAC molecular weight is higher than about 110K. It is interesting that the PDMDAAC fraction with M_w = 110K has a hydrodynamic size of ~9 nm,[47] which is also the size of free TX100–SDS micelles, as previously shown[36] or as obtained by dynamic light scattering results, discussed below.

The information from turbidity measurements provides the range of Y for soluble complex formation. The light scattering results presented below are all from systems with Y = 0.30 and 0.4 M NaCl.

Figure 2 shows the dependence on PDMDAAC molecular weight of R_h of the PDMDAAC/TX100–SDS complex as well as that of the accompanying unbound micelles from CONTIN analysis of the dynamic light scattering results. The R_h value of *ca.* 9 nm for free micelles is in agreement with previous results.[34] The size of the complex increases with increasing PDMDAAC molecular weight, while the size of the free TX100–SDS micelles remains essentially unchanged.

Figure 3 shows the dependence of R_h for complex and for PDMDAAC (without TX100–SDS) on PDMDAAC molecular weight. The R_h values of the complexes are about twice those of the PDMDAAC from which they are formed. Figure 4a shows some representative angular distribution of scattered intensity from complexes, and Figure 4b presents similar double-logarithmic plots for

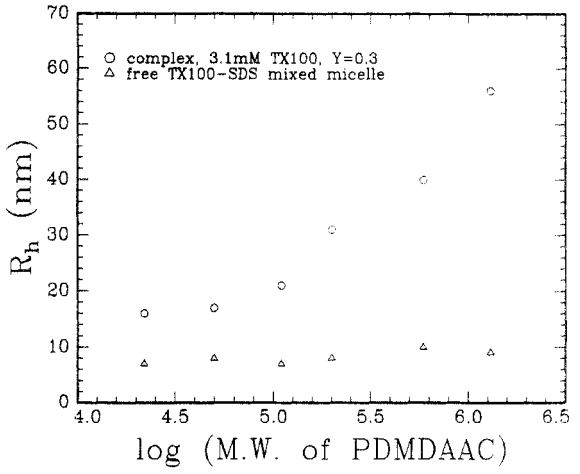

Figure 2. R_h of the complex and the free micelles from dynamic light scattering and CONTIN analysis. Two distribution peaks were observed from CONTIN analysis, one assigned to complex, the other to free micelles.

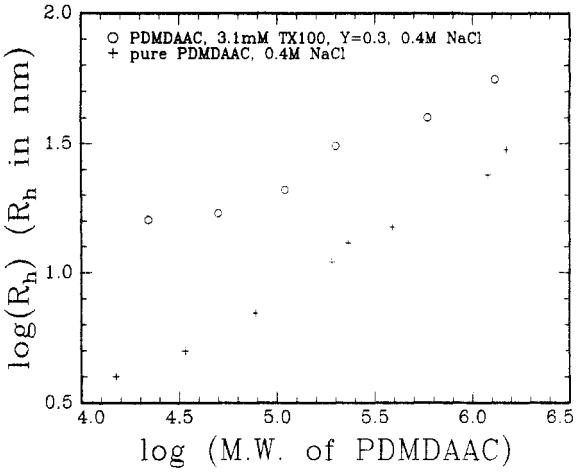

Figure 3. Dependence of R_h of complex upon PDMDAAC molecular weight. For comparison, the R_h values of pure PDMDAAC (without TX100 and SDS) are also shown.

R_g.[54] Interestingly, the R_g values are very close to those of the pure PDMDAAC fractions. This indicates that the overall PDMDAAC conformation does not change much upon complex formation; i.e., no significant chain expansion occurs. TX100–SDS micelles appear to occupy the space between the PDMDAAC segments. It is known that such a process will increase R_h because mobile solvent molecules inside the PDMDAAC coils are replaced by bound, immobile micelles, while the geometric R_g, which is largely dependent upon the topological conditions, remains largely unchanged.[55] Therefore, the complex formed is very compact, a conclusion also drawn earlier by Dubin and co-workers from light scattering measurements of Merquat 100/TX100–SDS.[35,36] Chu and coworkers observed similar phenomena:[56] for the bovine serum albumin (BSA)–polysaccharide conjugate, they found that the molecular weight of the conjugate (3500K) was about 7 times larger than that of the pure polymer (530K), yet R_g values were comparable: $R_g \sim 54$ nm for the conjugate and ~50 nm for the polymer.

The reason for the compact structure of the complex formed between polyelectrolyte and oppositely charged mixed micelles may be discussed in terms of thermodynamic quantities. Complex formation could be controlled by at least four factors. One is the electrostatic interaction between polyelectrolyte and oppositely charged mixed micelles. This enthalpy change is the main driving force

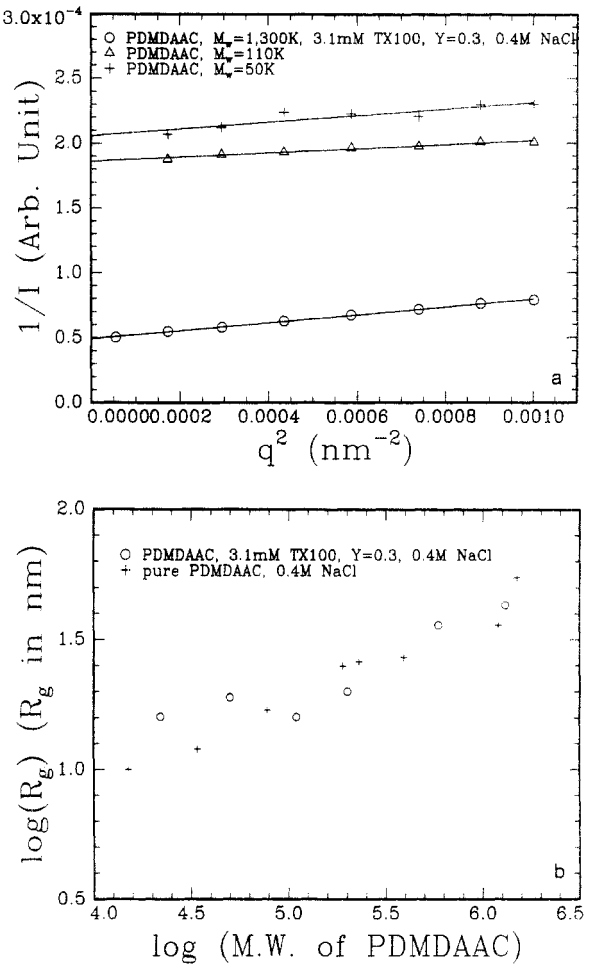

Figure 4. (a) Representative angular distribution of scattered intensity from complexes. (b) Dependence of R_g of complex on PDMDAAC molecular weight. For comparison, the R_g values of pure PDMDAAC without TX100 and SDS are also shown.

for complex formation and depends strongly upon the structure of polyelectrolyte and micelles, ionic strength, and temperature. On the other hand, binding gives rise to an entropy loss of the polyelectrolyte chains, ΔS_{config}. This loss may be compensated, to some extent, by the release of bound counterions from micelle and polyion. ΔS_{config} increases with increasing flexibility of the polyelectrolyte chains (note that the flexibility also depends upon the ionic strength). If a polyelectrolyte is already rather rodlike, this loss will not be significant. ΔS_{config} will be minimized if the binding takes place in such a way that the polyelectrolyte chain conformation remains largely unchanged during complex formation. The third factor is the excluded volume effect (steric effect) of the bulky micelles, which tends to expand the polyelectrolyte chain. The magnitude of this factor increases with micelle size. In a system where only *monomeric* surfactant is involved, as is the case in most literature research, this factor should not be significant. The fourth factor is the electrostatic repulsion of bound micelles given that the binding of micelles to the polyelectrolyte chain is unlikely to neutralize the charge on the micelle surface completely. This factor has an effect similar to micelle excluded volume on complex structure but depends strongly upon ionic strength. The final structure of the complex depends upon the relative magnitude of these four factors.

In the present system of PDMDAAC/TX100–SDS in 0.4 M NaCl, the electrostatic repulsion among bound micelles is probably not a significant factor because of the high ionic strength. The conformation of PDMDAAC in

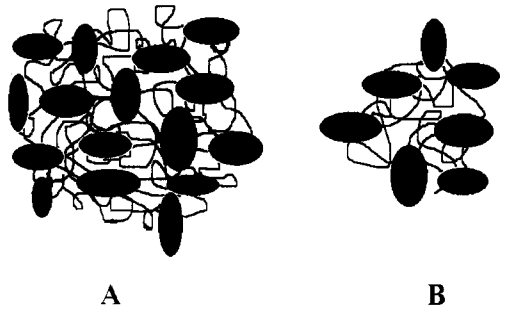

Figure 5. Simplified diagram of complexes formed from high molecular weight PDMDAAC (A) and low molecular weight PDMDAAC (B).

0.4 M NaCl is close to that of a flexible random coil.[48] Therefore, it is likely that the final structure of the complex in the present system depends upon the excluded volume factor and the entropy loss factor. The compact structure of the complex suggested by Figures 3 and 4 points to the entropy factor; i.e., the PDMDAAC chain tries to retain the original overall conformation during complex formation to minimize entropy loss, and the micelles tend to occupy the space between PDMDAAC chains. The excluded volume effect can also be seen from Figures 3 and 4; i.e., the overall slope of the curves is decreased upon complex formation. This tendency is more obvious at low PDMDAAC molecular weight, and there appears to be a transition point around PDMDAAC M_w = 110K, in agreement with the turbidity results. With decreasing molecular weight, the size of PDMDAAC becomes comparable to or even smaller than that of the micelles. The micelles cannot stay inside the PDMDAAC chain domain without large perturbation of the chain conformation. Thermodynamically, the most favorable case is for some of the bound micelles to reside at the outside boundary of the PDMDAAC domain. In this case, the total number of such "distal" bound micelles is likely to be greater for high molecular weight PDMDAAC due to the larger accessible space. But if this number is divided by the number of PDMDAAC repeating unit, the number of micelles bound per PDMDAAC repeating unit should be larger for low molecular weight PDMDAAC fractions, which gives rise to larger increase in both R_h and R_g. A depiction of complexes formed from high and low molecular weight PDMDAAC fractions is shown in Figure 5.

Figure 6 compares the CONTIN distribution of complex formed from polydisperse Merquat 100 with that from a PDMDAAC fractions. Qualitatively, the two complex peaks are similar. This can again be explained from the dependence of complex size upon PDMDAAC molecular weight indicated in Figure 3, which suggests that lower molecular weight fractions do not form low molecular weight complex.

Figure 7 shows the effect of C_p on R_h and R_g of the complex for the 590K fraction. With increasing C_p, R_h and R_g change very little until $z \equiv w_{PDMDAAC}/w_{surfactant} \approx 0.028$. Above 0.028, R_h and R_g increase sharply. It is noted that z = 0.09 corresponds to a 1:1 charge ratio of PDMDAAC to TX100–SDS.

Figure 8 shows the excess scattered intensity (extrapolated to $q \rightarrow 0$) of the complex as a function of z. After subtraction of the contribution from the mixed micelles, the values of I below z = 0.028 approach zero as $z \rightarrow 0$. This suggests that our use of scattered intensity from a polymer-free solution as the background correction is a good approximation.

Figure 8 shows a linear dependence on C_p of the excess scattered intensity from complexes up to z = 0.028, at which point the slope increases sharply. Consideration of Figure 8 along with Figure 7 indicates that below z = 0.028, only intrapolymer complexes are formed. The number of complexes increases with increasing z, while the size and the molar mass of complexes remain unchanged. Above z = 0.028, interpolymer complexes start to form. Both

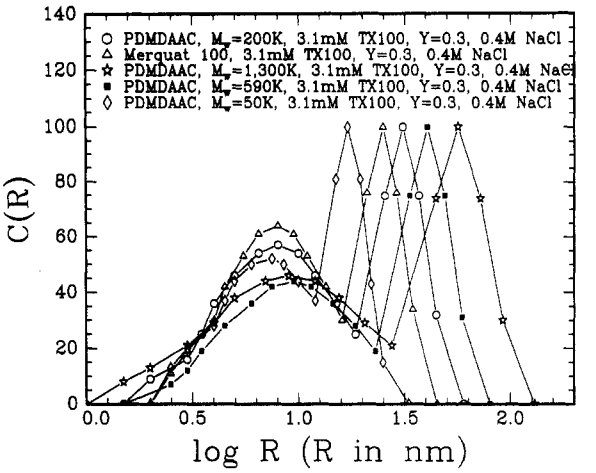

Figure 6. CONTIN distribution of the PDMDAAC/TX100–SDS system using Merquat 100 and PDMDAAC fractions. $C(R)$ is the scattered intensity averaged distribution of effective radius R. The peaks on the left are designated as from free micelles and those on the right, from complexes.

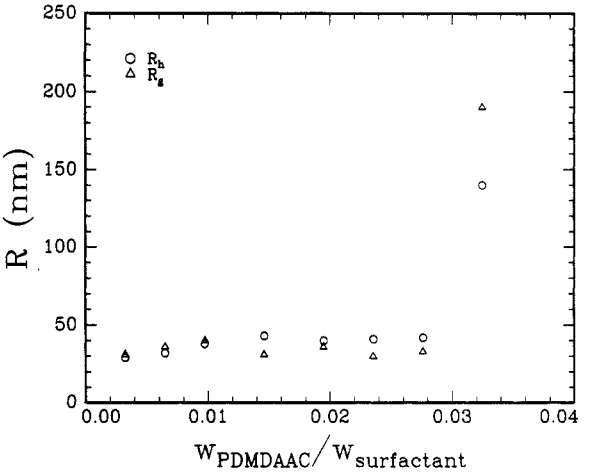

Figure 7. Dependence of R_h and R_g of complex upon PDMDAAC(M_w=590K) concentration expressed as the weight ratio of PDMDAAC to surfactant, z, at [TX100] = 3.1 mM, Y = 0.3, and in 0.4 M NaCl.

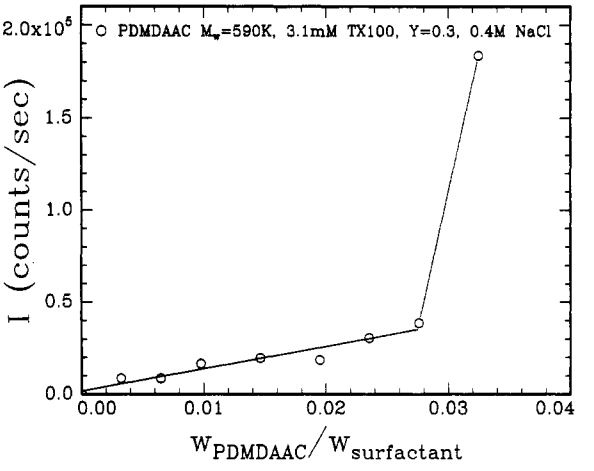

Figure 8. Excess scattered intensity (from extrapolation $q \rightarrow 0$) of complex as a function of z (PDMDAAC(M_w=590K)).

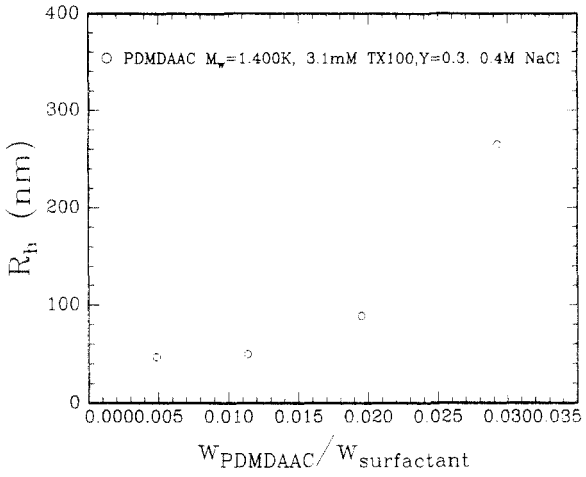

Figure 9. Dependence of R_h of complex upon z (PDMDAAC-(M_w=1400K)).

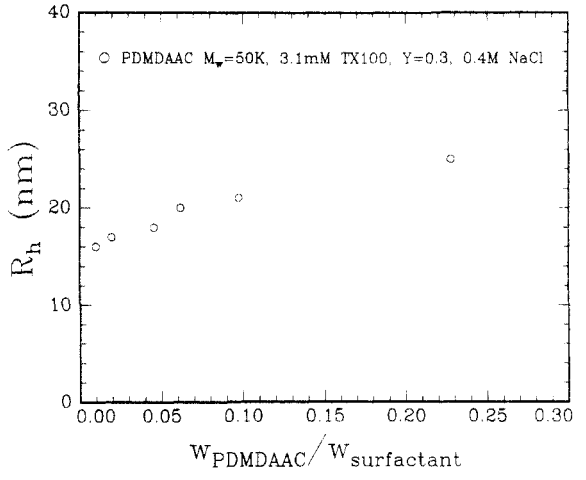

Figure 10. Dependence of R_h of complex upon z (PDMDAAC-(M_w=50K)).

the size and the molar mass of the complexes increase sharply. Furthermore, the solution above $z = 0.028$ is not very stable and "associative phase separation", a term introduced by Piculell,[4] may take place. The reason for associative phase separation might be the high molar mass and large size of the interpolymer complexes. We believe that such interpolymer complex formation is the precursor of associative phase separation, in this case corresponding to liquid–liquid phase separation ("complex coacervation").

Figure 9 shows that interpolymer complexes form at lower $z \cong 0.015$ for higher molecular weight (1400K) PDMDAAC. However, as seen in Figure 10, if the molecular weight of PDMDAAC is reduced to 50K, we could not observe the sharp transition. Figure 11 shows for this polymer an approximately linear increase in the excess scattered intensity from complexes with increasing z up to 0.21 (however, the excess scattered intensity is now only a rough estimate since at $z = 0.21$, the surfactant is not in large excess). R_h for this PDMDAAC fraction is around 6 nm,[48] even smaller than that of the mixed micelles (~9 nm). Therefore, we can speculate in the following way. For this low molecular weight PDMDAAC fraction, complex formation is more like an adsorption of PDMDAAC chains to the surface of micelles. It is difficult to imagine that one such small PDMDAAC macromolecule could bind many larger micelles; more likely, several macromolecules adsorb on the surface of a single micelle. This may be described as a multipolymer complex to distinguish it from the aforementioned interpolymer

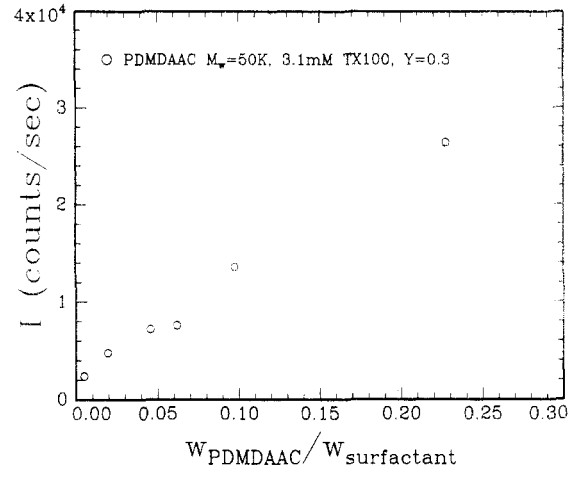

Figure 11. Excess scattered intensity (from extrapolation $q \rightarrow 0$) of complex as a function of z (PDMDAAC(M_w=50K)).

complex. The short PDMDAAC chain makes the formation of interpolymer complex of high molar mass and large size less probable. Multipolymer complexes are thus still small enough to be stable in solution without associative phase separation. We believe that this observation could explain the low recovery ratio of protein in polyelectrolyte–protein phase separation when a low molecular weight polyelectrolyte is used.[42-45] In other words, interpolymer complex formation may be necessary for a high recovery ratio.

Concluding Remarks

This paper elucidates the effect of polyelectrolyte molecular weight and polyelectrolyte concentration on complex formation with mixed micelles. The light scattering results indicate that the complexes are very compact. With increasing polyelectrolyte concentration, intrapolymer complexes change to interpolymer complexes, which appear to be precursors of associative phase separation (coacervation). Although polyelectrolyte molecular weight is not a significant factor for the structure of complex in the intrapolymer complex region, the intra- to interpolymer complex transition depends strongly upon the polyelectrolyte molecular weight; i.e., the polyelectrolyte concentration at which the transition occurs decreases with increasing polyelectrolyte molecular weight. If the polyelectrolyte molecular weight is low enough, high molar mass interpolymer complexes cannot be observed and associative phase separation does not occur. This may explain why high molecular weight polyelectrolyte is preferred for high protein recovery ratio based on polyelectrolyte–protein complex formation.

Acknowledgment. The support of Grant DMR9311433 from the National Science Foundation is gratefully acknowledged. We thank Yingfan Wang for his assistance with the GPC characterization of the PDMDAAC fractions.

References and Notes

(1) Robb, I. D. In *Anionic Surfactants, Physical Chemistry of Surfactant Action*; Lucassen-Reynders, E. H., Ed.; Marcel Dekker: New York, 1981; p 109.
(2) Goddard, E. D. *Colloids Surf.* **1986**, *19*, 301.
(3) Hayakawa, K.; Kwak, J. C. T. In *Cationic Surfactants. Physical Chemistry*; Rubingh, D. N., Holland, P. M., Eds.; Marcel Dekker: New York, 1991; Chapter 5, p 189.
(4) Piculell, B.; Lindman, B. *Adv. Colloid Interface Sci.* **1992**, *41*, 149.

(5) Lindman, B.; Thalberg, K. In *Interactions of Surfactants with Polymers and Proteins*; Goddard, E. D., Ananthapadmanabhan, K. P.; Ed.; CRC Press: Boca Raton, 1993; Chapter 5.
(6) Lindman, B.; Khan, A.; Marques, E.; Miquel, M.; Piculell, L.; Thalberg, K. *Pure Appl. Chem.* **1993**, *65*, 953.
(7) Goddard, E. D. *J. Soc. Cosmet. Chem.* **1990**, *41*, 23.
(8) Li, Y.; Dubin, P. L. In *Rheology of Surfactant Solutions*; Herb, C. A., Prud'homme, R. K., Eds.; American Chemical Society: Washington, DC, in press.
(9) Hayakawa, K.; Kwak, J. C. T. *J. Phys. Chem.* **1982**, *86*, 3866.
(10) Thalberg, K.; Lindman, B.; Bergfeldt, K. *Langmuir* **1991**, *7*, 2893.
(11) Abuin, E. B.; Scaiano, J. C. *J. Am. Chem. Soc.* **1984**, *106*, 6274.
(12) Almgren, M.; Hansson, P.; Mukhtar, E.; van Stam, J. *Langmuir* **1992**, *8*, 2405.
(13) Chu, D.-Y.; Thomas, J. K. *J. Am. Chem. Soc.* **1986**, *108*, 6270.
(14) Thalberg, K.; van Stam, J.; Lindblad, C.; Almgren, M.; Lindman, B. *J. Phys. Chem.* **1991**, *95*, 8975.
(15) Chandar, P.; Somasundaran, P.; Turro, N. J. *Macromolecules* **1988**, *21*, 950.
(16) Herslöf, A.; Sundelöf, L.; Edsman, K. *J. Phys. Chem.* **1992**, *96*, 2345.
(17) Kawabata, N.; Hayashi, T.; Nishikawa, M. *Bull. Chem. Soc. Jpn.* **1986**, *59*, 2861.
(18) Cesarano, J., III; Aksay, I. A. *J. Am. Ceram. Soc.* **1988**, *71*, 1062.
(19) Margolin, A.; Sherstyuk, S. F.; Izumrudov, V. A.; Zezin, A. B.; Kabanov, V. A. *Eur. J. Biochem.* **1985**, *146*, 625.
(20) Clark, K. M.; Glatz, C. E. *Biotechnol. Prog.* **1987**, *3*, 241.
(21) Fisher, R. R.; Glatz, C. E. *Biotechnol. Bioeng.* **1988**, *32*, 777.
(22) Bozzano, A. G.; Andrea, G.; Glatz, C. E. *J. Membr. Sci.* **1991**, *55*, 181.
(23) Dubin, P. L.; Strege, M. A.; West, J. In *Large Scale Protein Purification*; Ladish, M., Ed.; American Chemical Society: Washington, DC, 1990; Chapter 5.
(24) Shaner, S. L.; Melancon, P.; Lee, K. S.; Burgess, M. T.; Record, M. T., Jr. *Cold Spring Harbor Symp. Quant. Biol.* **1983**, *47*, 463.
(25) von Hippel, P. H.; Bear, D. G.; Morgan, W. D.; McSwiggen, J. A. *Annu. Rev. Biochem.* **1984**, *53*, 389.
(26) Goddard, E. D.; Hannan, R. B. *J. Colloid Interface Sci.* **1976**, *55*, 73.
(27) Ohbu, K.; Hiraishi, O.; Kashiwa, I. *J. Am. Oil Chem. Soc.* **1982**, *59*, 108.
(28) Dubin, P. L.; Oteri, R. *J. Colloid Interface Sci.* **1983**, *95*, 453.
(29) Dubin, P. L.; Davis, D. D. *Macromolecules* **1984**, *17*, 1294.
(30) Dubin, P. L.; Davis, D. D. *Colloids Surf.* **1985**, *13*, 113.
(31) Dubin, P. L.; Rigsbee, D. R.; McQuigg, D. W. *J. Colloid Interface Sci.* **1985**, *105*, 509.
(32) Dubin, P. L.; Rigsbee, D. R.; Gan, L.-M.; Fallon, M. A. *Macromolecules* **1988**, *21*, 2555.
(33) Dubin, P. L.; Thé, S. S.; McQuigg, D. W.; Chew, C. H.; Gan, L.-M. *Langmuir* **1989**, *5*, 89.
(34) Dubin, P. L.; Vea, M. E.; Fallon, M. A.; Thé, S. S.; Rigsbee, D. R.; Gan, L.-M. *Langmuir* **1990**, *6*, 1422.
(35) Dubin, P. L.; Thé, S. S.; McQuigg, D. W.; Gan, L.-M.; Chew, C. H. *Macromolecules* **1990**, *23*, 2500.
(36) Xia, J.; Zhang, H.; Rigsbee, D. R.; Dubin, P. L.; Shaikh, T. *Macromolecules* **1993**, *26*, 2759.
(37) The effect of the molecular weight of nonionic polymers on polymer–surfactant complex formation has been reviewed by Goddard[38] and by Lindman and co-workers.[5] Generally, a minimum nonionic polymer molecular weight is required for complex formation. Above this value, a weaker interaction could be observed. However, it has to be noted that, although the techniques used are similar, complex formation from nonionic polymers and surfactants may be very different from that from polyelectrolytes and oppositely charged surfactants. The complex from nonionic polymers and charged surfactants has a charge accumulation, while the complex formation from polyelectrolytes and oppositely charged surfactants involves charge neutralization. The driving force for the two is thus different.
(38) Goddard, E. D. *Colloids Surf.* **1986**, *19*, 255.
(39) Dubin, P. L.; Chew, C. H.; Gan, L.-M. *J. Colloid Interface Sci.* **1989**, *128*, 566.
(40) Thalberg, K.; Lindman, B.; Karlström, G. *J. Phys. Chem.* **1991**, *95*, 3370.
(41) Choi, L.; Kim, O. *Langmuir* **1994**, *10*, 57.
(42) Sternberg, M.; Hershberger, D. *Biochim. Biophys. Acta* **1974**, *342*, 195.
(43) Sakamoto, M.; Kuramoto, N.; Komiyama, J.; Iijima, T. *Int. J. Biol. Macromol.* **1982**, *4*, 207.
(44) Kuramoto, N.; Sakamoto, M.; Komiyama, J.; Iijima, T. *Int. J. Biol. Macromol.* **1984**, *6*, 69.
(45) Shieh, J.; Glatz, C. E. In *Macromolecular Complexes in Chemistry and Biology*; Dubin, P. L., Bock, J., Davis, R. M., Schultz, D., Thies, C., Eds.; Springer-Verlag: New York, 1994; p 273.
(46) Cabane, B.; Duplessix, R. *J. Phys. (Paris)* **1982**, *43*, 1529.
(47) Dubin, P. L.; Principi, J. M.; Smith, B. A.; Fallon, M. A. *J. Colloid Interface Sci.* **1989**, *127*, 558.
(48) Xia, J.; Dubin, P. L.; Edwards, S.; Havel, H. A. *J. Polym. Sci.*, accepted.
(49) Chu, B. *Laser Light Scattering*; Academic *Press*: New York, 1991.
(50) Berne, B. J.; Pecora, R. *Dynamic Light Scattering*; Wiley: New York, 1976.
(51) Schmitz, K. S. *An Introduction to Dynamic Light Scattering by Macromolecules*; Academic Press: Boston, 1990.
(52) Provencher, S. W. *J. Chem. Phys.* **1976**, *64*, 2772; *Makromol. Chem.* **1979**, *180*, 201.
(53) Stockmayer, W. H.; Schmidt, M. *Pure Appl. Chem.* **1982**, *54*, 407; *Macromolecules* **1984**, *17*, 509.
(54) In general, R_g values below 10 nm are not obtained with a useful level of precision; two observations[48] support the significance of R_g measured for the low molecular weight fractions here. (1) The R_g/R_h ratio is constant for all fractions in the 10K–100K molecular weight range, and (2) the correlation between log R_g and log M is consistently good in this same range.
(55) Wachenfeld-Eisele, E.; Burchard, W. In *Biological and Synthetic Networks*; Kramer, O., Ed.; Elsevier: Amsterdam, 1988; p 305.
(56) Patkowski, A.; Bujalowski, W.; Chu, B.; Schneerson, R.; Robbins, J. B. *Biopolymers* **1982**, *21*, 1503.